Arch. Metall. Mater. **71** (2026), 1, 93-105

DOI: https://doi.org/10.24425/amm.2026.157773

KRISHNA MURTHY PALANKI[1*], VENKATA SUBBAIAH KAMBAGOWNI[2]

THE INFLUENCE OF Co-CROSS LINKED STARCH ON THERMAL, IMPACT, MORPHOLOGICAL AND MECHANICAL CHARACTERISTICS OF POLYLACTIC ACID/MODIFIED STARCH BLENDS TREATED WITH POLYETHYLENE GLYCOL 400

This study focuses on the development of biodegradable polylactic acid (PLA)/modified starch (MS) biocomposites, employing polyethylene glycol 400 (PEG) as a plasticizer via a melt compounding method. To improve the hygroscopic characteristics, native potato starch undergoes modification via co-crosslinking with glyoxal and ammonium zirconium carbonate (AZC). Loadings of modified starch at 10, 20, and 30 wt.% were integrated with PEG at 4, 7, and 10 wt.% in PLA. The analysis focused on the thermal, morphological, tensile, and impact properties. The thermal study indicates that, without any change in thermal stability, the crystallinity percentage of the composites increased by 53% when the modified starch loading was raised to 30%. The SEM images of the fragmented samples reveal the presence of modified starch pullouts and deformation bands, which can be linked to the elevated plasticizer content. The analyses of tensile and impact properties reveal improved ductility and impact resistance associated with increased PEG content. The findings reveal that the composite with 7% PEG and 20% MS (G7S20) exhibited the most notable improvement in properties when compared to pure PLA.

Keywords: Plasticizer; Biocomposites; Polylactic acid (PLA); Potato starch; polyethylene glycol 400 (PEG)

1. Introduction

Contemporary existence has grown progressively dependent on plastics, known for their affordability, resilience, and lightness. Plastics, made from synthetic or semi-synthetic polymers, can be shaped into numerous forms, making them suitable for diverse applications. Plastics are everywhere in our daily lives, found in packaging materials like bottles, bags, and containers that ensure the safe storage and transport of goods [1]. Plastic packaging provides superior barrier properties against moisture, gases, and contaminants, thereby preserving product integrity and extending shelf life [2]. Nonetheless, the worldwide dependence on plastics has resulted in significant environmental challenges, such as waste management difficulties, microplastic pollution, and the increase of landfills [3].

Polylactic acid (PLA) is a biodegradable aliphatic polyester that can completely break down into non-toxic metabolites in both aerobic and anaerobic conditions. When compared to conventional petroleum-based polymers, PLA exhibits advantageous tensile strength and effective water vapor barrier properties. Despite its notable strength, its application is constrained by its cost and fragile nature [4,5]. Therefore, suitable fillers [6,7] and modifiers [8] should be employed to overcome the limitations. Among the available fillers, potato starch stands out as a cost-effective, naturally occurring polymer that can be hydrolyzed into glucose. This material acts as a filler due to its binding characteristics with PLA, resulting in decreased material expenses. In its fundamental state, potato starch demonstrates certain limitations, including brittleness, low tensile strength, and hydrophilic properties [9,10]. Consequently, native starch is treated with appropriate plasticizers to enhance processing properties and attain a uniform amorphous structure, leading to the development of thermoplastic starch (TPS) [11]. Even in its thermoplastic state, the water-absorbing characteristics of starch lead to inadequate interfacial adhesion among the materials, resulting in a reduction of their properties [12,13]. To improve the interfacial interaction between the materials, Polyethylene glycol 400 (PEG) is utilized as a modifier [14-16]. Even with the addition of PEG, the hydrophilic nature of the starch remains a significant challenge that affects the properties of the composites [10,14]. Co-cross linking is a chemical modification process that entails the concurrent application of multiple

[1] DEPARTMENT OF MECHANICAL ENGINEERING, ENGINEERING AND TECHNOLOGY PROGRAM, GVP COLLEGE FOR DEGREE AND P.G.COURSES (A), VISAKHAPATNAM, ANDHRA PRADESH, INDIA
[2] DEPARTMENT OF MECHANICAL ENGINEERING, ANDHRA UNIVERSITY COLLEGE OF ENGINEERING (A), ANDHRA UNIVERSITY, VISAKHAPATNAM, ANDHRA PRADESH, INDIA
* Corresponding author:krishnapalanki26@gmail.com

linking agents to create a complex and dense molecular network [17]. To improve the hydrophobic properties of thermoplastic starch, it undergoes dual crosslinking with suitable chemicals [18]. The hydrophobic characteristics of thermoplastic starch are improved via co-crosslinking with AZC and glyoxal [19,20].

Consequently, the existing literature indicates that there has been minimal research on the combination of co-cross-linked starch with PLA in the presence of PEG. This investigation focused on the formulation of composites using PLA as the matrix, with co-cross linked potato starch incorporated at various weight percentages as the filler, alongside polyethylene glycol 400 introduced at different weight percentages as the plasticizer.

2. Materials and methodology

2.1. Materials

PLA pellets of Luminy-175 were provided by Tahim Industries (Delhi, India) and serve as the matrix material, while potato starch (soluble) co-crosslinked with AZC and glyoxal acts as the filler. PEG serves as a plasticizer. TABLE 1 presents the specifications of the materials utilized.

2.2. Experimentation

The biocomposite of PLA/MS/PEG is created by first transforming native potato starch into a thermoplastic form, and then modifying it through co-crosslinking with appropriate chemicals. Potato starch is treated with water at high temperatures to transform it into a thermoplastic state [21]; the resulting thermoplastic starch is co-crosslinked with AZC and glyoxal at a concentration of 5 wt.% [20]. The composite pellets, featuring an L/D ratio of 20, are manufactured via melt compounding with a co-rotating twin screw extruder. The operation occurs at a torque of 100 N-m, with feeder temperatures recorded at 100°C, 170°C, 160°C, 165°C, and 180°C, all under a pressure of 300 bar [22]. Tensile (ASTM D638, Type I) and impact (ASTM D256) specimens are fabricated utilizing a vertical injection moulding apparatus at a temperature of 200°C and a pressure of 20 kPa. TABLE 2 presents the composition of the composites.

2.3. Characterization of thermal and mechanical properties

Prior to the tests, the injection molded samples underwent exposure in a hot air oven at 60°C for a duration of 24 hours to mitigate atmospheric moisture. The study focuses on the thermal and mechanical properties. The fractured impact specimens are analyzed using a Scanning Electron Microscope (SEM) (Carl Zeiss Evo MA 15) to conduct fractography. The tensile behavior of the composites is evaluated using a universal testing machine (Instron Make) at room temperature, utilizing a 10 kN load cell and a speed rate of 10 mm/min.

X-Ray Diffraction (XRD) analysis was conducted to examine the crystal structure of the polymers, specifically pure PLA and PLA/PEG/MS composites, utilizing a Bruker D8 advance machine with Cu-kα radiation (λ = 0.1542 nm). The diffraction data is collected within a 2θ range of 0° to 60°. The scanning rate is set at 0.05° s^{-1} and the step size is 0.5 s.

The Attenuated total reflectance – Fourier transform infrared (ATR-FTIR) spectrophotometer (spectrum-II, Bruker corporation) is utilized to record the ATR-FTIR spectra of Pure PLA and PLA/PEG/MS biocomposites. The specimens undergo scanning at a frequency ranging from 500 to 4000 cm^{-1}, with a scan rate set at 4 cm^{-1}.

The thermal behavior of the PLA biocomposite specimens was examined in accordance with the ASTM D3418 standard, utilizing a differential scanning calorimeter (DSC) (TA, USA, DSCQ20). The measurement was conducted under two heating cycles for an approximately 15 mg sample at a rate of 10°C/min, with a temperature range from 30°C to 300°C. During the sec-

TABLE 1

Properties of the materials

Name of the Material	Chemical formulae	Density	Phase
Pure PLA	$(C_3H_4O_2)_n$	1.24	Solid pellets form
Potato Starch	$(C_6H_{10}O_5)_n$	0.55	White powdery form
Polyethylene glycol 400	$C_{2n}H_{4n+2}O_{n+1}$ n = 8.2 to 9.1	1.12	Liquid
Ammonium Zirconium carbonate	$C_2H_2O_8Zr_2H_4N$	1.38	Liquid
Glyoxal 40%	$C_2H_2O_2$	1.24	Liquid

TABLE 2

Designation of the composites and their composition

S. No	Name of the specimen	MS (wt.%)	PEG (wt.%)	PLA (wt.%)
1	P100 (Pure PLA)	0	0	100
2	G4S10	10	4	86
3	G4S20	20	4	76
4	G4S30	30	4	66
5	G7S10	10	7	83
6	G7S20	20	7	73
7	G7S30	30	7	63
8	G10S10	10	10	80
9	G10S20	20	10	70
10	G10S30	30	10	60

ond heating cycle, the thermal variables such as glass transition temperature (T_g), cold crystallization temperature (T_{cc}), melting temperature (T_m), cold crystallization enthalpy (ΔH_{cc}), and fusion enthalpy (ΔH_m) were determined by analysing the corresponding peak and area under the curve. Additionally, based on the previous study carried out by Y. Dong et al. [23], the percentage of crystallinity (χ_c) assessment was conducted using DSC analysis as outlined in Eq. (1). The investigation of thermal stability and decomposition was conducted through thermogravimetric analysis (TGA) using a Q50 from TA Instruments. The analysis was performed at a scan rate of 10°C/min, covering a temperature range from 0°C to 800°C. The thermal weight loss and the corresponding derivative temperature have been documented.

3. Results and discussions

3.1. Examination of microstructures

Fig. 1(a-i) presents the scanning electron microstructures of the fractured samples for the composite blends. The fractography of the specimens demonstrates the presence of deformation bands marked by a decrease in modified starch content, showcasing notable agglomeration of modified starch in various sizes along with the existence of pores within the matrix material. The deformation bands seen in the shattered specimens demonstrate the ductile properties of the composite material. The white

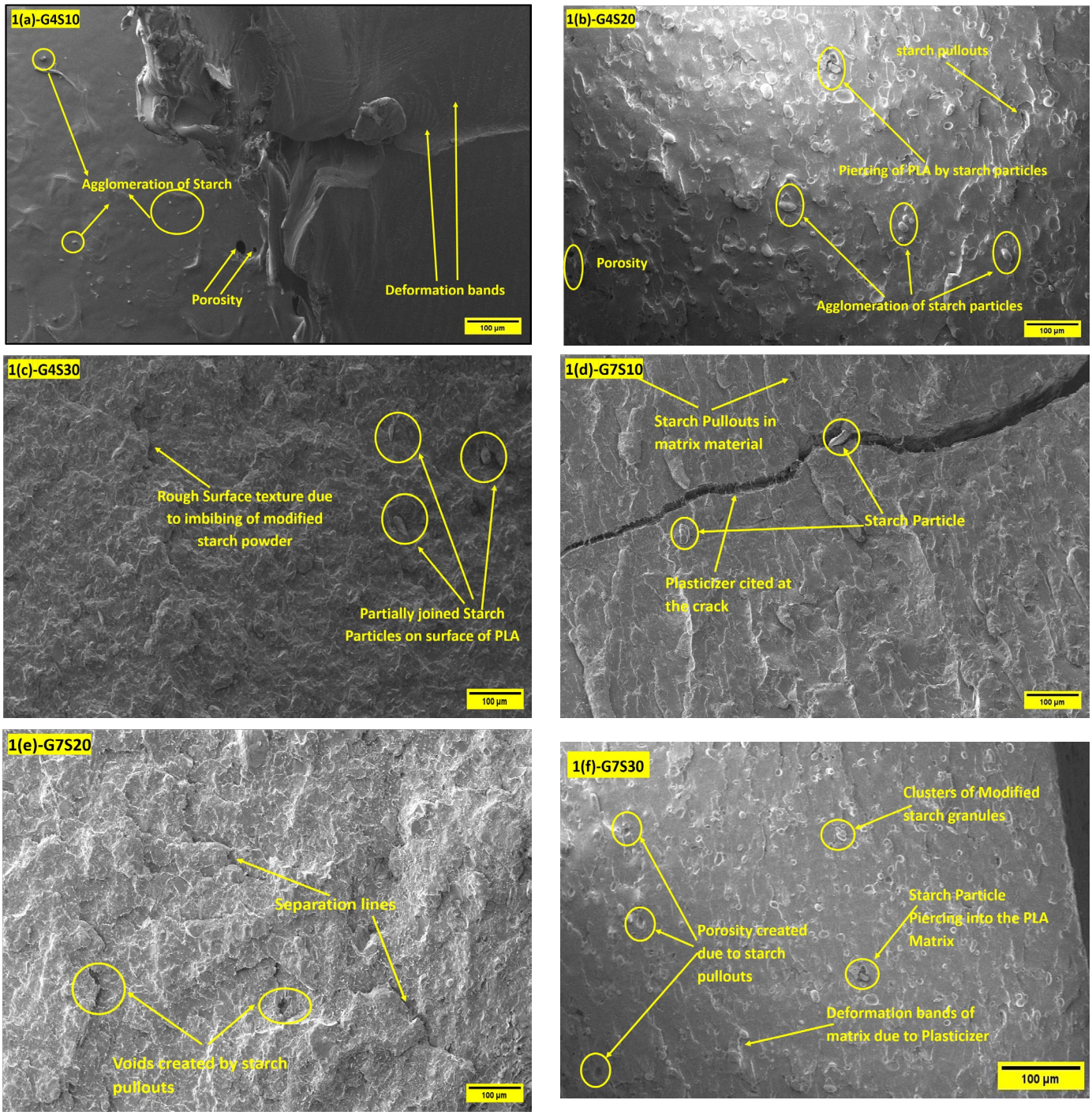

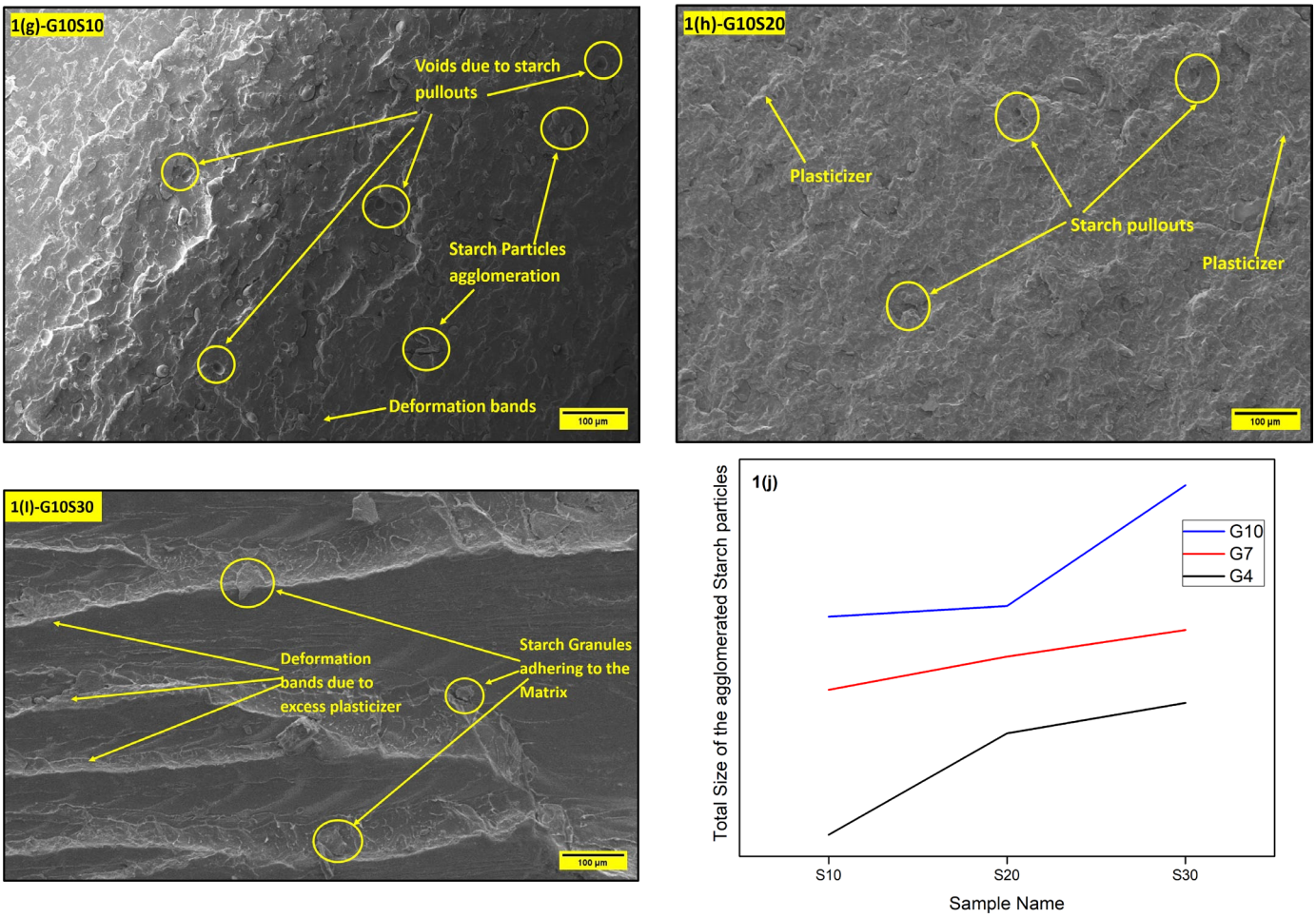

Fig. 1. Microstructures of fractured specimens: (a) G4S10, (b) G4S20, (c) G4S30, (d) G7S10, (e) G7S20, (f) G7S30, (g) G10S10, (h) G10S20, (i) G10S30; (j) Total Size of the Starch Agglomeration with increase in starch content

layered lines indicate the presence of a plasticizer. The rise in modified starch loading in PLA led to an uneven distribution and clustering of the modified starch granules within the PLA matrix. The observed increase in size of the agglomerated starch granules correlates with the plasticizer content, as demonstrated in Fig. 1(j). An average of 15% rise in the size of agglomerated starch granules is observed. Given that PLA and starch are inherently distinct materials characterized by contrasting polarities, this often results in thermodynamic immiscibility. Despite incorporating PEG 400, the insufficient interfacial interactions among these materials led to the formation of voids, resulting in starch agglomerations and pullouts [24,25].

3.2. Tensile investigations

The evaluation of mechanical properties such as tensile strength, percentage of elongation, and Young's modulus is conducted for the prepared PLA/PEG/MS biocomposites. The measurement was performed on three distinct times and the mean value has been documented in TABLE 3. At modified starch concentrations of 10 wt.%, an increase in PEG content led to enhanced elongation at break, as illustrated in Fig. 2; however, this was accompanied by a twofold reduction in tensile strength and modulus. The observed enhanced elongation can be attributed to the permeation occurring among the polymer chains of PLA, which reduces intermolecular forces and enhances chain mobility. The improved chain mobility leads to a decrease in cohesion, subsequently resulting in a reduction of tensile strength [26]. This result is more advantageous in comparison to earlier investigations [24,27-30]. However, the rate at which the properties degraded decreased with an increase in the content of modifying starch. Xue Ping and Wang indicated that the decrease in properties of the composites compared to pure PLA results from the reaction between the hydroxyl group of PEG and the carboxyl group of PLA, which enhances interfacial adhesion [31].

3.3. Impact studies

The impact strength of the polymer blends is evaluated through the Izod method utilizing the IT 504 PLASTIC IMPACT machine, following the ASTM D256 Standard. TABLE 3 presents the mean value derived from three samples. Zhang and Liang et.al demonstrated that PEG improves the molecular mobility of the matrix, alters the crystallinity of PLA, and leads

TABLE 3

Tensile and impact results of polymer composite blends

S. No	Name of the specimen	Young's Modulus (GPA)	Tensile Strength (MPa)	Percentage of Elongation (%)	Impact Strength (J/m)
1	Pure PLA	2.523±0.0598	63.95±0.142	6.802±0.569	28.57±0.125
2	G4S10	2.484±0.0185	**43.66±0.274**	9.354±0.629	34.90±0.72
3	G4S20	**2.799±0.0239**	40.50±0.270	7.250±0.531	29.49±1.50
4	G4S30	2.747±0.0347	33.74±0.316	4.844±0.752	33.28±1.41
5	G7S10	1.805±0.0617	36.00±0.320	158.323±6.78	33.06±3.83
6	G7S20	1.944±0.0230	31.37±0.250	**113.677±12.55**	40.58±3.71
7	G7S30	1.794±0.0340	27.34±0.368	81.621±12.25	38.41±3.15
8	G10S10	1.198±0.0392	25.91±0.840	230.833±12.29	46.75±3.22
9	G10S20	1.252±0.0227	23.68±0.360	227.120±3.87	**62.83±4.64**
10	G10S30	1.195±0.0318	22.56±0.614	223.520±2.62	60.26±3.15

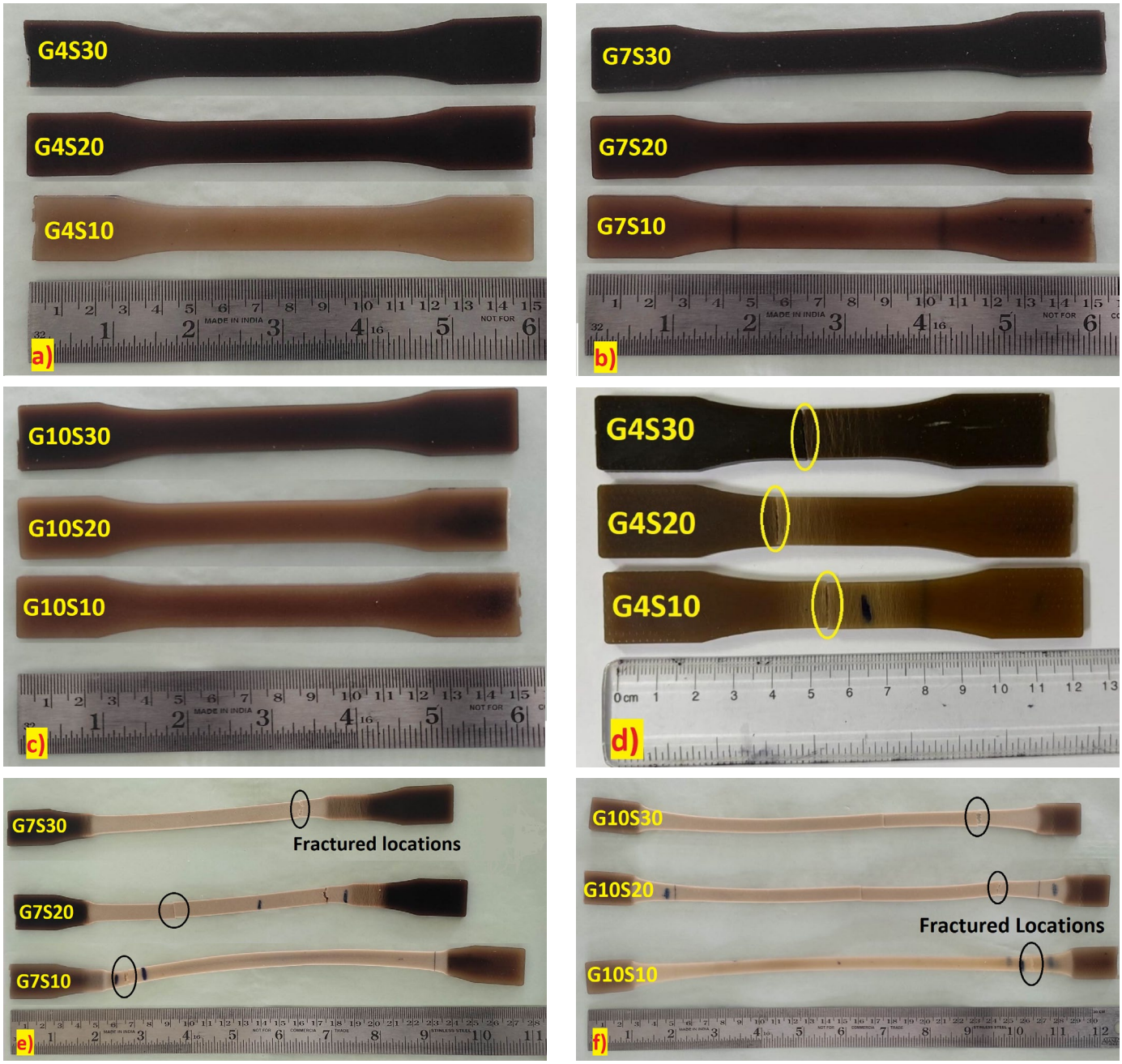

Fig. 2. Samples before tensile test: a) (G4S10, G4S20 and G4S30), b) (G7S10, G7S20 and G7S30), c) (G10S10, G10S20 and G10S30). Fractured Specimens after tensile testing: d) (G4S10, G4S20 and G4S30), e) (G7S10, G7S20 and G7S30), f) (G10S10, G10S20 and G10S30)

to an enhancement in impact strength [32]. A comparable result is observed when the PEG content falls below 5%, showing a slight enhancement in impact strength averaging 14%. When the PEG content surpasses 5%, a notable increase of 120% in impact strength is observed at 10% PEG content in conjunction with 20% modified starch (G10S20). Increasing the PEG 400 content boosts chain mobility, which leads to a reduction in the glass transition temperature, thus allowing the composite to absorb more energy during impact. Moreover, an increase in PEG fosters improved crystallinity, which may facilitate structural reorganization (resulting in finer and more uniform spherulite components), thereby enhancing the effective dissipation of impact energy [33].

3.4. DSC Examination of PLA/MS/PEG biocomposites

The evaluation of thermal phase transition properties was conducted using the differential scanning calorimetry thermograms (DSC) illustrated in Fig. 3(a-d), with the relevant data summarized in TABLE 4. The observation indicated a decrease in T_g for the PLA/PEG/MS biocomposites. The decrease indicates that the addition of the plasticizer creates free volume by reducing intermolecular forces, thus facilitating the movement of PLA molecules, which may lead to improved miscibility within the composite. The thermal properties of the PLA/PEG/MS biocomposites exhibited a decrease in T_g (maximum 9°C for G7S30) when compared to pure PLA. Considering that starch shows reduced thermal stability compared to PLA, an increase in the modified starch content could result in a decrease in T_g, potentially facilitating accelerated thermal degradation of the composites due to the disruption of bond stability [34,35]. The addition of plasticizer (PEG) probably diminishes intermolecular entanglement within PLA chains, thereby increasing the free volume and promoting molecular motion.

The decrease in T_{cc} of the composites compared to pure PLA suggests that crystallization takes place at reduced temperatures, thereby improving the flexibility of the molecular chains. This adaptability promotes the development of chain segments de-

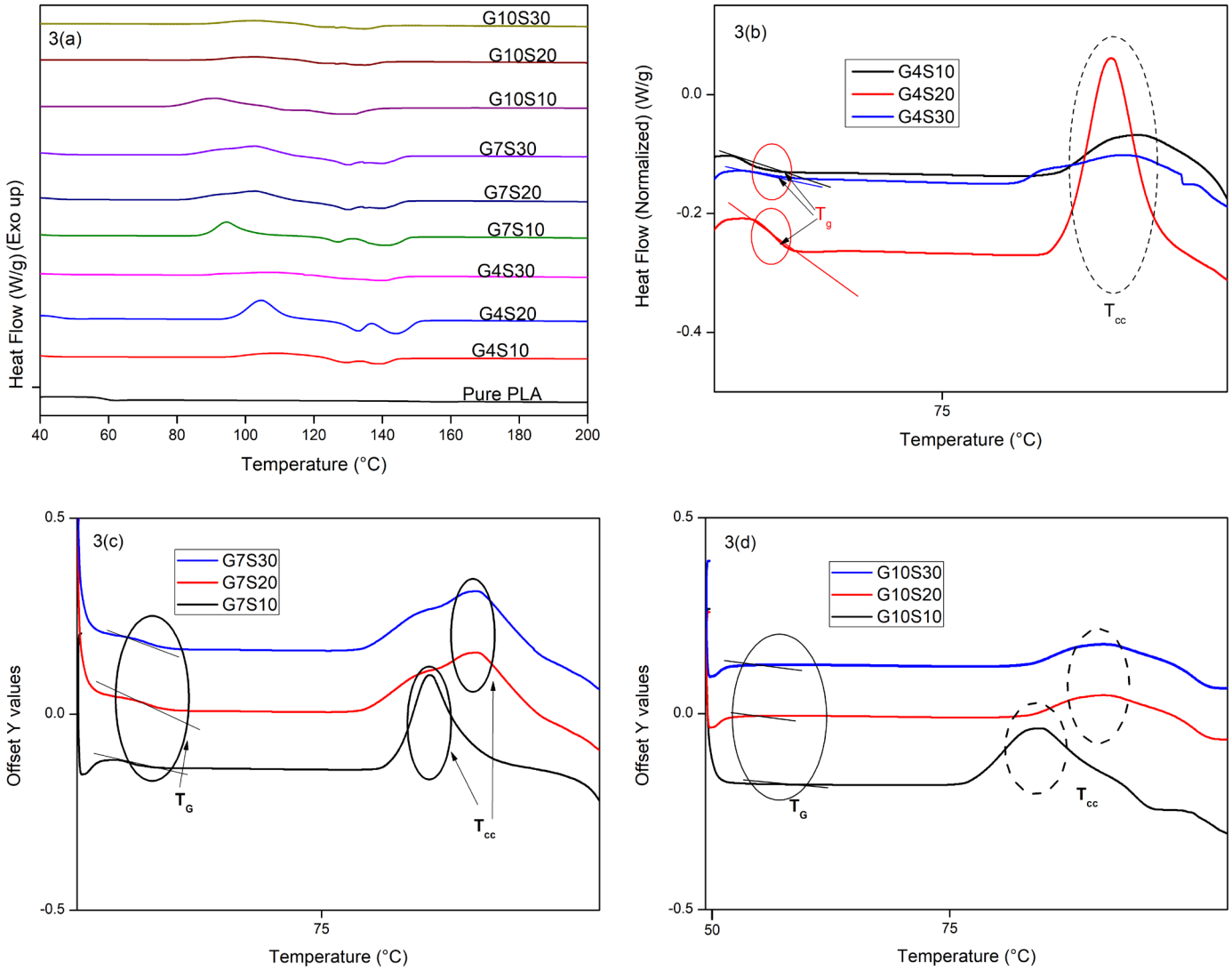

Fig. 3. (a) DSC thermograms of the second heating cycle of pure PLA and PLA/PEG/MS biocomposites; DSC thermograms of the second heating cycle of: (b) G4S10, G4S20 and G4S30, (c) G7S10, G7S20 and G7S30, (d) G10S10, G10S20 and G10S30

TABLE 4

Thermal characteristics of the second heating cycle of pure PLA, PLA/PEG/MS composites at various PEG and MS loadings

S. No	Name of the specimen	T_g (°C)	T_{cc} (°C)	ΔH_{cc} (J/g)	ΔH_m (J/g)	χ_c (%)
1	Pure PLA	61.19	155.16	2.95	6.44	3.73
2	G4S10	56.78	128.57	3.11	6.51	4.23
3	G4S20	55.00	132.74	3.19	6.54	4.70
4	G4S30	54.37	139.8	3.26	6.79	5.71
5	G7S10	56.45	127.67	3.13	6.58	4.44
6	G7S20	54.73	129.61	3.22	6.61	4.96
7	G7S30	52.62	128.37	3.50	6.84	5.66
8	G10S10	56.07	128.92	3.29	6.43	4.19
9	G10S20	55.78	135.63	3.35	6.51	4.82
10	G10S30	54.18	127.9	3.80	6.81	5.36

rived from modified starch, resulting in an enhanced degree of crystallinity [36]. The calculation of the degree of crystallinity for the composites follows Eq. (1), indicating that pure PLA demonstrates a low crystallinity of 3.73%. A rise in modified starch and PEG is associated with a noted enhancement in crystallinity. In their study Blázquez-Blázquez et al. reported that incorporating a plasticizer enhances nucleation, which in turn increases chain mobility and improves crystallinity [37]. From TABLE 4 it is observed that there is a slight increase in thermal energy (ΔH_m) and crystallinity with the rising content of modified starch. T. Ke et al in their study indicated that starch acts as a nucleating agent during thermal treatment, resulting in improved crystallization of PLA [30]

$$\chi_c = \frac{\Delta H_m - \Delta H_{cc}}{\Delta H_m^0} \times \frac{100}{1 - w_f} \quad (1)$$

Where ΔH_m and ΔH_{cc} represents the enthalpy of melting and cold crystallization. ΔH_m is enthalpy of melting for 100% crystalline PLA ($\Delta H_m^0 = 93$ J/g [38]) $(1 - w_f)$ represents the remaining weight percentage of the PLA in the prepared composite.

Miftahul et al. in their study noted that the enhanced crystallinity is associated with increased stability, indicating that a greater amount of energy is necessary to disturb the crystalline structure [39]. The enhancement in impact strength of the composites, as indicated in TABLE 3, reflects an improvement in the crystal structure.

3.5. TGA and DTG Analysis of PLA/MS/PEG biocomposites

The thermal stability and decomposition of the prepared composites are examined through Thermogravimetric Analysis (TGA) performed in a nitrogen atmosphere at a heating rate of 10°C/min. The thermograms of the prepared biocomposites are illustrated in Fig. 4, showcasing the TGA and DTG results.

The thermal degradation of pure PLA begins at temperatures exceeding 300°C due to the back biting intermolecular transesterification reaction [40,41]. From TABLE 5 it is observed that, in the context of a 10% weight loss, a rise in modified starch content is associated with a reduction in decomposition temperature. Earlier studies have indicated a comparable trend for PLA-related biocomposites [42,43]. The diminished thermal stability of the composites can be linked to the decreased thermal degradation of the plasticized starch [44].

The first derivative curves of the TGA thermographs (DTG) reveal that all PLA/PEG/MS composites exhibits a singular peak, indicating that the main degradation transpires in a unified step. From TABLE 5 it is observed that the maximum temperature for biodegradation (T_{max}) of the PLA/PEG/MS composites is less than that of pure PLA. This decrease is due to the reduced molecular weight of starch and PEG, which interferes with the PLA chains. Pal and Katiyar et.al noted a similar decrease in maximum temperature in their study [45]. The data presented in TABLE 5 demonstrates a notable improvement in T_{max} for the G4S30 composite. Nonetheless, an increase in modified starch content is linked to an enhancement in, indicating better resistance to thermal breakdown of the composites. The improvement in thermal breakdown resistance could be attributed to the addition of modified starch, which demonstrates enhanced barrier properties via dual cross-linking that limits heat transfer [46,47]. The final analysis revealed that the remaining weight

TABLE 5

TG and DTG data of Pure PLA and PLA/PEG/MS composites

S. No	Name of the specimen	$T_{10\%}$ (°C)	$T_{50\%}$ (°C)	$T_{90\%}$ (°C)	T_{max} (°C)	T_{offset} (°C)	Remaining weight %
1	Pure PLA	334.94	359.93	374.79	365.460	452.84	0.00622
2	G4S10	306.95	340.07	366.49	354.490	457.13	0.02987
3	G4S20	305.33	340.19	365.82	359.650	470.69	0.04203
4	G4S30	277.48	352.57	362.94	369.340	486.83	0.04263
5	G7S10	297.19	339.74	373.41	341.580	456.49	0.03274
6	G7S20	296.56	338.61	363.53	351.910	462.64	0.04619
7	G7S30	294.25	336.25	360.88	362.560	469.31	0.04845
8	G10S10	267.54	331.64	373.18	331.770	451.22	0.04585
9	G10S20	266.23	328.80	371.82	333.180	460.36	0.04675
10	G10S30	261.66	325.16	366.24	335.410	465.13	0.04754

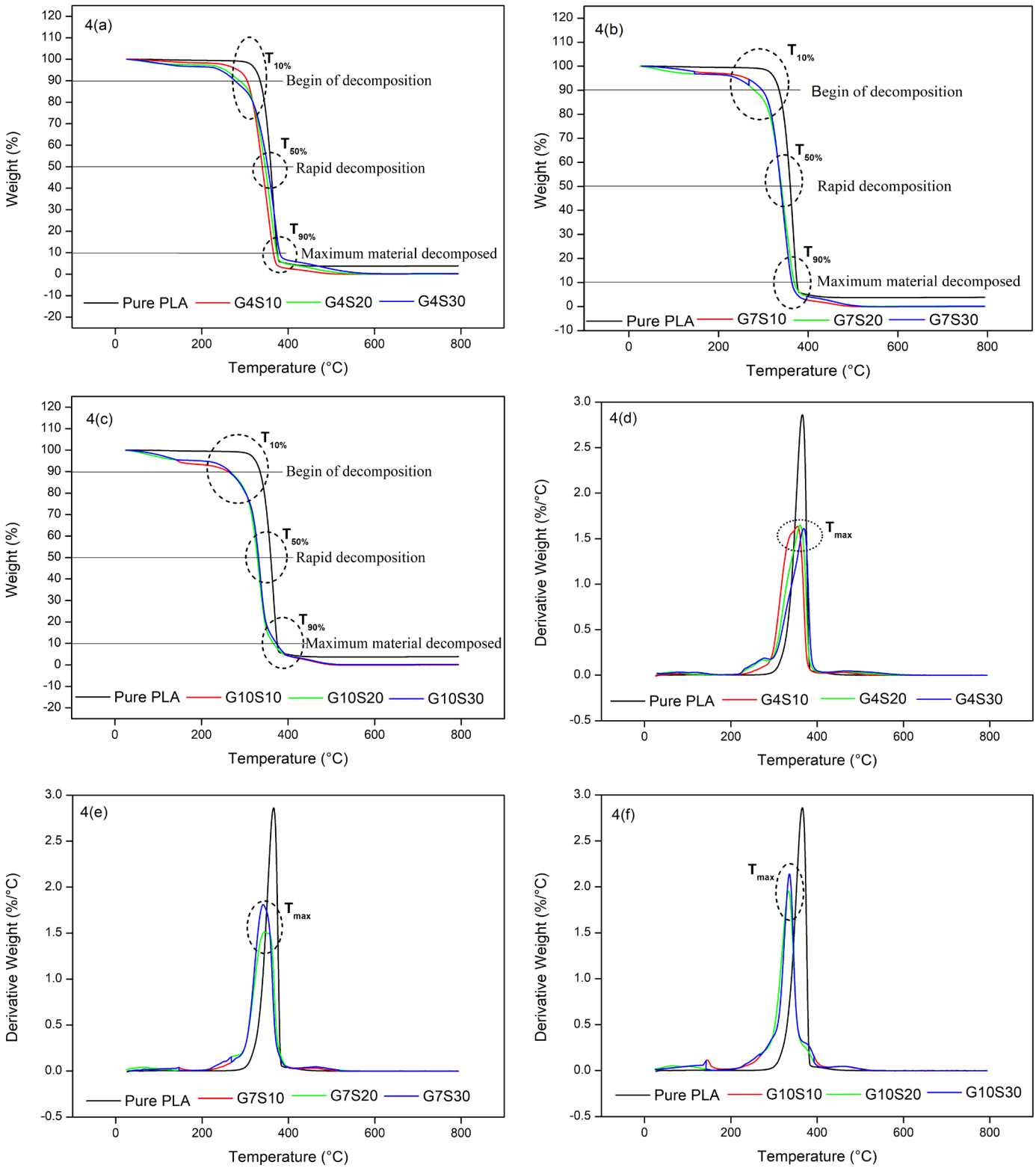

Fig. 4. TGA thermograms for Pure PLA: (a) G4S10, G4S20, and G4S30, (b) G7S10, G7S20 and G7S30, (c) G10S10, G10S20 and G10S30. DTG thermograms for Pure PLA: (d) G4S10, G4S20 and G4S30, (e) G7S10, G7S20 and G7S30, (f) G10S10, G10S20 and G10S30

percentage of the composites rose with an increase in modified starch content. As noted by Laurence McKeen et al. [48], the increased crystallinity in the composites may somewhat limit molecular movement, potentially explaining this enhancement. As the concentration of PEG increases, which enhances molecular mobility, the T_{max} and T_{offset} values decrease.

3.6. X-Ray Diffraction Analysis

Fig. 5 presents the diffractograms obtained for pure PLA and PLA/PEG/MS composites. A distinct peak appears at a 2θ value of approximately 16.7°, which aligns with the orthorhombic α-crystalline phase (planes of (1 1 0) and (2 0 0)) of PLA [49].

In all composites, the primary peak position remains consistent, suggesting that the crystal structure of the PLA is not notably modified. Potato starch generally displays B type hexagonal crystallites, which are marked by significant peaks at 5.5°, 17°, 19.5°, 22°, and 24° [47]. Minor peaks appear at $2\theta \approx 19.7°$, suggesting the presence of modified starch [50,51]. The results indicate that modified starch is incorporated into the PLA matrix, contrasting with findings from similar studies that utilized the melt compounding technique [47]. The current study indicates that no associated secondary major peaks have been identified. As a result, this study finds that the melt compounding technique applied for PLA/PEG/MS effectively facilitated the efficient blending of modified starch within the PLA matrix. TABLE 4 illustrates the enhancement in the crystal structure of the composites, as derived from the DSC thermograms.

3.7. Fourier transform infrared spectroscopy (FTIR)

The chemical structures of the biocomposites were examined through ATR-FTIR, as shown in Fig. 6(a-c). Fig. 6 (a-c) shows that for pure PLA, the stretching of the ester-carbonyl (C=O) occurs at an absorption band of 1748 cm^{-1}, while the ester linkage (C-O-C) is observed at 1452 cm^{-1} and 1182 cm^{-1}. The stretching vibrations of C-H bonds are noted at 2996.7 cm^{-1}, 2945.7 cm^{-1}, and 2879.5 cm^{-1} [16,52]. The IR spectrum of the blended composites shows a band within the range of 3000 cm^{-1} to 3600 cm^{-1}, which becomes more pronounced with increased concentrations of modified starch, suggesting effective blending of modified starch with PLA [52]. An intensity peak at 1084 cm^{-1} suggests the presence of PEG, which becomes more pronounced with an increase in PEG content, attributed to the C–O–C ester stretching bands of PEG. The intensity evolutions at 1748 cm^{-1} presented in Fig. 7 reveal a growing trend corresponding to the increase in PEG content, suggesting the compatibility between PLA and PEG. An elevation in PEG content results in a higher terminal hydroxyl fraction, which fosters robust intermolecular hydrogen bonding between PLA and PEG, subsequently leading to an increase in the peak [53,54].

The Carboxyl group (-COO-) of PLA showed a trend of increasing intensity at the absorption band of 1508 cm^{-1} with the rising content of modified starch, where the peak area at 1508 cm^{-1} increased by an average of 30%, attributed to asymmetric stretching [55]. In conclusion, the integration of modified starch content with the PLA matrix was successfully achieved based on the supplied feed.

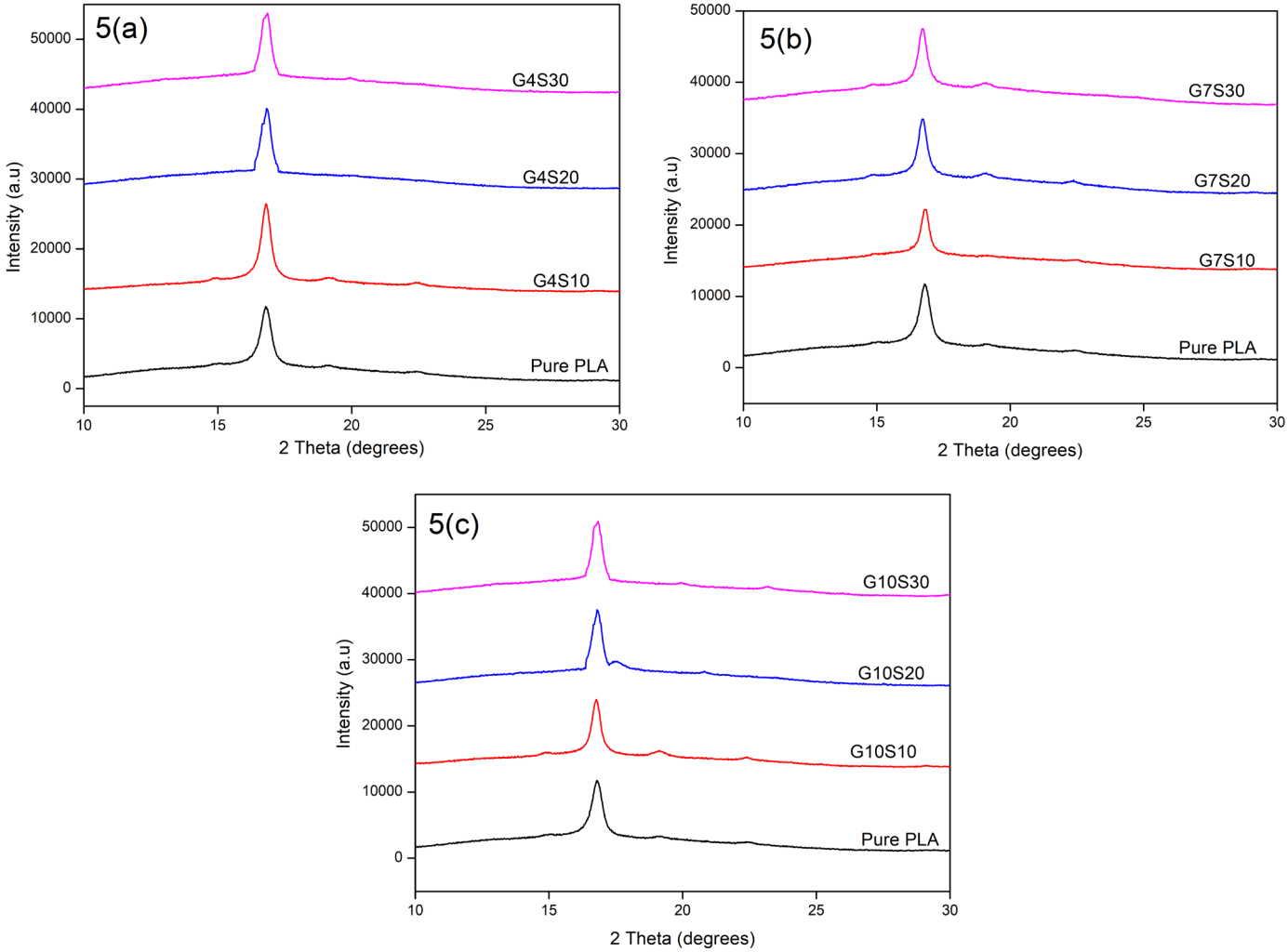

Fig. 5. XRD diffractograms of PLA: (a) G4S10, G4S20 and G4S30, (b) G7S10, G7S20 and G7S30, (c) G10S10, G10S20 and G10S30

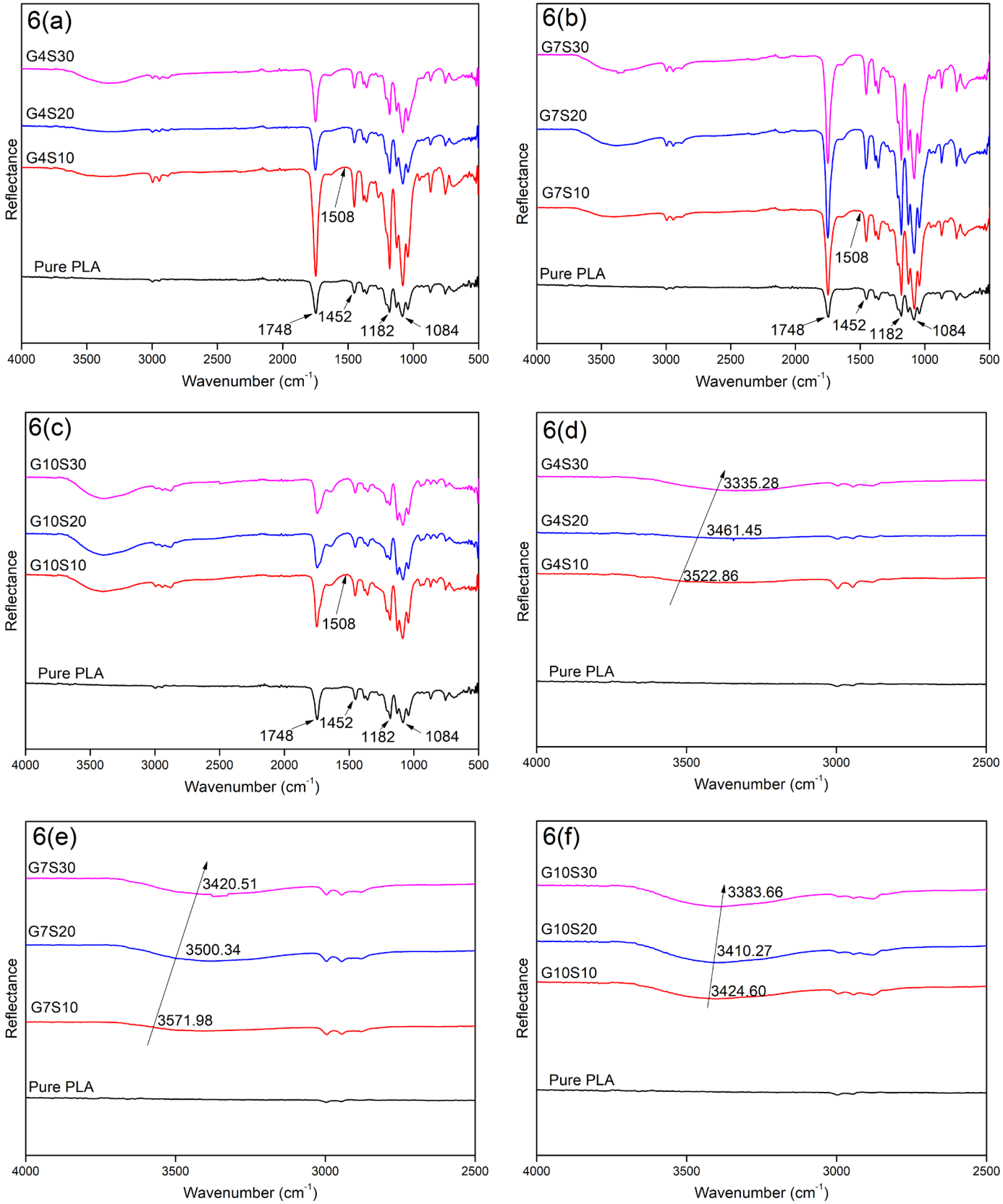

Fig. 6. ATR-FTIR Spectra of Pure PLA: (a) G4S10, G4S20 and G4S30, (b) G7S10, G7S20 and G7S30, (c) G10S10, G10S20 and G10S30. ATR-FTIR expanded hydroxyl regions of Pure PLA: (d) G4S10, G4S20 and G4S30, (e) G7S10, G7S20 and G7S30, (f) G7S10, G7S20 and G7S30

The hydroxyl regions of ATR-FTIR, as illustrated in Fig. 6(d-f), indicate that the wavenumbers of the hydroxyl (-OH) group of PLA decreased by approximately 125 cm^{-1} on average with an increase in modified starch content. The decrease in wavenumber suggests that a blend has formed between the carbonyl group of PLA and the hydroxyl groups of modified starch [56-58].

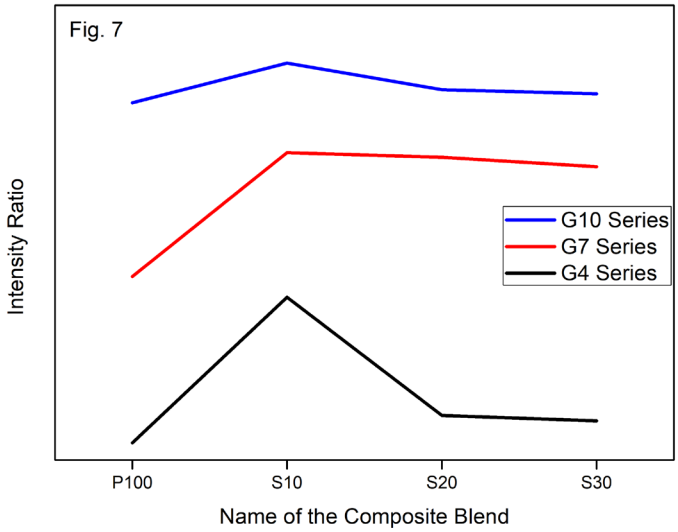

Fig. 7. Intensity ratios of PLA/PEG/MS biocomposites

4. Conclusions

This investigation effectively produced PLA-based biocomposites through melt compounding, utilizing modified starch as a reinforcement and PEG as a plasticizer. The FTIR analysis provided clear evidence of the interaction between PLA and modified starch, indicated by a reduction in the wavenumber of the hydroxyl groups. The improved crystallinity of the PLA matrix, as verified by XRD and DSC, was linked to the nucleating influence of modified starch. Nonetheless, this effect lessened when the PEG content surpassed 7%.

The TGA analysis indicated that the thermal degradation resistance of the biocomposites enhanced with a higher modified starch content, with the G4S30 formulation demonstrating superior stability compared to pure PLA. With PEG content surpassing 7%, the degradation peaks were observed to shift to lower temperatures, signifying a reduction in the thermal stability of the biocomposite.

The SEM analysis indicated a restricted phase compatibility between PLA and modified starch, resulting in the emergence of small starch clusters and voids. Despite this, the tensile properties exhibited a distinct trade-off: ultimate tensile strength and Young's modulus diminished with higher modified starch content, with G4S10 and G4S20 identified as optimal, while elongation at break and impact strength enhanced, pointing to G7S20 and G10S20 as their optimal values. In a similar manner, increased PEG content improved ductility while compromising strength.

In summary, through the optimization of modified starch and PEG content, biocomposites that exhibits a well-balanced and satisfactory blend of mechanical and thermal properties are developed. The resulting material shows a slightly improved crystal structure and adequate ductility, positioning it as a feasible and sustainable option for certain single-use packaging applications.

5. Future Scope

The current study faces limitations due to insufficient compatibility between PLA and MS, along with reduced thermal stability. Consequently, future investigations are to focus on utilizing compatibilizers to improve compatibility. Furthermore, the biodegradation rate and the identification of the optimal blend for the prepared composites are to be carried out using multi-criteria decision-making techniques.

REFERENCES

[1] P. Singh, V.P. Sharma, Integrated plastic waste management: environmental and improved health approaches. Procedia Environ. Sci. **35**, 692-700 (2016). DOI: https://doi.org/10.1016/j.proenv.2016.07.068

[2] R. Auras, B. Harte, S. Selke, An overview of polylactides as packaging materials. Macromol. Biosci. **4**, 835-864 (2004). DOI: https://doi.org/10.1002/mabi.200400043

[3] I.S. Oberoi, P. Rajkumar, S. Das, Disposal and recycling of plastics. Mater. Today Proc. **46**, 7875-7880 (2021). DOI: https://doi.org/10.1016/j.matpr.2021.02.562

[4] N.K. Kalita, M.K. Nagar, C. Mudenur, A. Kalamdhad, V. Katiyar, Biodegradation of modified poly(lactic acid) based biocomposite films under thermophilic composting conditions. Polym. Test. **76**, 522-536 (2019). DOI: https://doi.org/10.1016/j.polymertesting.2019.02.021

[5] J. Muller, C. González-Martínez, A. Chiralt, Combination of poly(lactic) acid and starch for biodegradable food packaging. Materials **10**, 952 (2017). DOI: https://doi.org/10.3390/ma10080952

[6] M. Ji, et al., Enhanced mechanical properties, water resistance, thermal stability, and biodegradation of the starch-sisal fibre composites with various fillers. Mater. Des. **198**, 109373 (2021). DOI: https://doi.org/10.1016/j.matdes.2020.109373

[7] V. Gigante, et al., Improvement of interfacial adhesion and thermomechanical properties of PLA based composites with wheat/rice bran. Polymers (Basel) **14**, 3389 (2022). DOI: https://doi.org/10.3390/polym14163389

[8] M. Asadollahi, et al., Improving mechanical properties and biocompatibility of 3D printed PLA by the addition of PEG and titanium particles. Bioprinting **27**, e00228 (2022). DOI: https://doi.org/10.1016/j.bprint.2022.e00228

[9] M.I. Din, T. Ghaffar, J. Najeeb, Z. Hussain, R. Khalid, H. Zahid, Potential perspectives of biodegradable plastics for food packaging application. Food Additives & Contaminants: Part A **37**, 665-680 (2020). DOI: https://doi.org/10.1080/19440049.2020.1718219

[10] Z.N. Diyana, et al., Physical properties of thermoplastic starch derived from natural resources and its blends. Polymers **13**, 1396 (2021). DOI: https://doi.org/10.3390/polym13091396

[11] A. Zarski, K. Bajer, J. Kapuśniak, Review of the most important methods of improving the processing properties of starch toward non-food applications. Polymers (Basel) **13**, 832 (2021). DOI: https://doi.org/10.3390/polym13050832

[12] N.F. Zaaba, H. Ismail, Tensile and morphological properties of poly(lactic acid)/thermoplastic starch blends. Polymer-Plastics Technology and Materials **58**, 1945-1964 (2019). DOI: https://doi.org/10.1080/25740881.2019.1599941

[13] S. Jayarathna, M. Andersson, R. Andersson, Recent advances in starch-based blends and composites for bioplastics applications. Polymers **14**, 4557 (2022). DOI: https://doi.org/10.3390/polym14214557

[14] S. Momeni, et al., Effect of poly(ethylene glycol) emulation on the degradation of PLA/starch composites. Polymers (Basel) **13**, 1019 (2021). DOI: https://doi.org/10.3390/polym13071019

[15] F. Hassouna, J.M. Raquez, F. Addiego, P. Dubois, V. Toniazzo, D. Ruch, New approach on the development of plasticized polylactide via reactive extrusion. Eur. Polym. J. **47**, 2134-2144 (2011). DOI: https://doi.org/10.1016/j.eurpolymj.2011.08.001

[16] M.M.F. Ferrarezi, M. de Oliveira Taipina, L.C.E. da Silva, M. do C. Gonçalves, Poly(ethylene glycol) as a compatibilizer for poly(lactic acid)/thermoplastic starch blends. J. Polym. Environ. **21**, 151-159 (2013). DOI: https://doi.org/10.1007/s10924-012-0480-z

[17] S. Punia Bangar, K.V. Sunooj, M. Navaf, Y. Phimolsiripol, W.S. Whiteside, Recent advancements in cross-linked starches for food applications. Int. J. Food Prop. **27**, 411-430 (2024). DOI: https://doi.org/10.1080/10942912.2024.2318427

[18] Z. Huang, et al., Mechanically robust dual-crosslinking elastomer enabled by a facile self-crosslinking approach. Materials **15**, 3983 (2022). DOI: https://doi.org/10.3390/ma15113983

[19] D. Song, V. Breedveld, Y. Deng, Rheological study of self-crosslinking and co-crosslinking of ammonium zirconium carbonate and starch in aqueous solutions. J. Appl. Polym. Sci. **122**, 1019-1029 (2011). DOI: https://doi.org/10.1002/app.34215

[20] S. Ni, et al., Glyoxal improved functionalization of starch with AZC enhances the hydrophobicity and strength of co-crosslinked polymer. Eur. Polym. J. **110**, 385-393 (2019). DOI: https://doi.org/10.1016/j.eurpolymj.2018.12.003

[21] C.Q. Yang, G.G. Xu, Y. Deng, Applications of bifunctional aldehydes to improve paper wet strength. J. Appl. Polym. Sci. **83**, 2539-2547 (2002). DOI: https://doi.org/10.1002/app.10195

[22] R. Salehiyan, S. Sinha Ray, Processing of polymer blends emphasizing melt compounding and reactive processing. Processing of Polymer-based Nanocomposites **278**, 167-197 (2018). DOI: https://doi.org/10.1007/978-3-319-97792-8_6

[23] Y. Dong, et al., Polylactic acid/halloysite nanotube composite mats: influence of nanotube content and modification. Compos. Part A Appl. Sci. Manuf. **76**, 28-36 (2015). DOI: https://doi.org/10.1016/j.compositesa.2015.05.011

[24] H. Sadeghi Ghari, H. Nazockdast, Morphology development and mechanical properties of PLA/plasticized starch blends. Polymer **245**, 124729 (2022). DOI: https://doi.org/10.1016/j.polymer.2022.124729

[25] S. Mangaraj, R.R. Thakur, A. Yadav, Development and characterization of PLA and cassava starch-based biodegradable film for food packaging. J. Food Process. Preserv. **46**, e16314 (2022). DOI: https://doi.org/10.1111/jfpp.16314

[26] J. Sringam, T. Kajornprai, T. Trongsatitkul, N. Suppakarn, Shape memory performance and microstructural evolution in PLA/PEG blends. Polymers **17**, 225 (2025). DOI: https://doi.org/10.3390/polym17020225

[27] M.A. Huneault, H. Li, Morphology and properties of compatibilized polylactide/thermoplastic starch blends. Polymer **48**, 270-280 (2007). DOI: https://doi.org/10.1016/j.polymer.2006.11.023

[28] T. Ke, S.X. Sun, P. Seib, Blending of poly(lactic acid) and starches containing varying amylose content. J. Appl. Polym. Sci. **89**, 3639-3646 (2003). DOI: https://doi.org/10.1002/app.12617

[29] B. Nagy, N. Miskolczi, Z. Eller, Improving mechanical properties of PLA/starch blends using masterbatch. Polymers **13**, 2981 (2021). DOI: https://doi.org/10.3390/polym13172981

[30] H. Hu, A. Xu, D. Zhang, W. Zhou, S. Peng, X. Zhao, High-toughness poly(lactic acid)/starch blends prepared through reactive blending. Molecules **25**, 5951 (2020). DOI: https://doi.org/10.3390/molecules25245951

[31] P. Xue, K. Wang, M. Jia, M. Yang, Biodegradation and mechanical property of polylactic acid/thermoplastic starch blends with polyethylene glycol. J. Wuhan Univ. Technol. Mater. Sci. Ed. **28**, 157-162 (2013). DOI: https://doi.org/10.1007/s11595-013-0658-9

[32] F.J. Li, S.D. Zhang, J.Z. Liang, J.Z. Wang, Effect of polyethylene glycol on the crystallization and impact properties of polylactide-based blends. Polym. Adv. Technol. **26**, 465-475 (2015). DOI: https://doi.org/10.1002/pat.3475

[33] S. Jia, D. Yu, Y. Zhu, Z. Wang, L. Chen, L. Fu, Morphology crystallization and thermal behaviors of PLA-based composites via GO/PEG. Polymers **9**, 528 (2017). DOI: https://doi.org/10.3390/polym9100528

[34] R. Acioli-Moura, X.S. Sun, Thermal degradation and physical aging of poly(lactic acid) and its blends with starch. Polym. Eng. Sci. **48**, 829-836 (2008). DOI: https://doi.org/10.1002/pen.21019

[35] L. Benkraled, et al., Effect of plasticization and annealing on thermal, dynamic mechanical, and rheological properties of poly(lactic acid). Polymers **16**, 974 (2024). DOI: https://doi.org/10.3390/polym16070974

[36] E.H. Backes, L. de N. Pires, L.C. Costa, F.R. Passador, L.A. Pessan, Analysis of the degradation during melt processing of PLA/biosilicate composites. J. Compos. Sci. **3**, 52 (2019). DOI: https://doi.org/10.3390/jcs3020052

[37] E. Blázquez-Blázquez, R. Barranco-García, T.M. Díez-Rodríguez, M.L. Cerrada, E. Pérez, Role of plasticizers on the crystallization of PLA and its composites. J. Mater. Sci. **59**, 6305-6321 (2024). DOI: https://doi.org/10.1007/s10853-024-09556-x

[38] J.F. Turner II, A. Riga, J. Zhang, J. Collis, Characterization of drawn and undrawn poly-L-lactide films by differential scanning calorimetry. J. Therm. Anal. Calorim. **75**, 257-268 (2004). DOI: https://doi.org/10.1023/b:jtan.0000017347.08469.b1

[39] S.Y. Massijaya, et al., Thermal properties enhancement of PLA–starch-based polymer composite using sucrose. Polymer **16**, 1028 (2024). DOI: https://doi.org/10.3390/polym16081028

[40] Y. Fan, H. Nishida, Y. Shirai, Y. Tokiwa, T. Endo, Thermal degradation behaviour of poly(lactic acid) stereocomplex. Polym. Degrad. Stab. **86**, 197-208 (2004).
DOI: https://doi.org/10.1016/j.polymdegradstab.2004.03.001

[41] Y. Wang, B. Steinhoff, C. Brinkmann, I. Alig, In-line monitoring of the thermal degradation of poly(L-lactic acid) during melt extrusion. Polymer **49**, 1257-1265 (2008).
DOI: https://doi.org/10.1016/j.polymer.2008.01.010

[42] N.F. Zaaba, H. Ismail, Influence of different compounding sequence and filler loading on properties of PLA/thermoplastic starch biocomposites. J. Vinyl Addit. Technol. **26**, 413-422 (2020).
DOI: https://doi.org/10.1002/vnl.21756

[43] J.R. Rodríguez-Núñez, et al., Evaluation of physicochemical and antifungal properties of polylactic acid–thermoplastic starch–chitosan biocomposites. Polym. Plast. Technol. Eng. **56**, 44-54 (2017). DOI: https://doi.org/10.1080/03602559.2016.1211683

[44] Y.A. Alassmy, et al., A green organocatalytic pathway for the preparation of esterified supercritical CO2-dried potato starch products. J. Appl. Polym. Sci. **140**, e53585 (2023).
DOI: https://doi.org/10.1002/app.53585

[45] A.K. Pal, V. Katiyar, Melt processing of biodegradable poly(lactic acid)/functionalized chitosan nanocomposite films. J. Polym. Res. **24**, 1305 (2017).
DOI: https://doi.org/10.1007/s10965-017-1305-5

[46] B. Wang, et al., Enhancing the mechanical and barrier properties of starch-based green packaging films via dual crosslinking. Carbohydr. Polym. **364**, 123787 (2025).
DOI: https://doi.org/10.1016/j.carbpol.2025.123787

[47] R.B. Valapa, G. Pugazhenthi, V. Katiyar, Effect of graphene content on the properties of poly(lactic acid) nanocomposites. RSC Adv. **5**, 28410-28423 (2015).
DOI: https://doi.org/10.1039/C4RA15669B

[48] L. McKeen, Introduction to the physical, mechanical, and thermal properties of plastics and elastomers. The Effect of Sterilization on Plastics and Elastomers 57-84 (2012).
DOI: https://doi.org/10.1016/B978-1-4557-2598-4.00003-4

[49] V.K. Thakur, D.J. Pochan, Poly(L-lactic acid)/layered silicate nanocomposite: fabrication, characterization, and properties. Chem. Mater. **15**, 2847-2855 (2003).
DOI: https://doi.org/10.1021/cm034369+

[50] L. Chen, Y. Tian, B. Sun, C. Cai, R. Ma, Z. Jin, Measurement and characterization of external oil in fried waxy maize starch granules. Food Chem. **242**, 131-138 (2018).
DOI: https://doi.org/10.1016/j.foodchem.2017.09.016

[51] J. Li, G.H. Shin, I.W. Lee, X. Chen, H.J. Park, Soluble starch formulated nanocomposite increases water solubility and stability of curcumin. Food Hydrocoll. **56**, 41-49 (2016).
DOI: https://doi.org/10.1016/j.foodhyd.2015.11.024

[52] Z.B. Cuevas-Carballo, S. Duarte-Aranda, G. Canché-Escamilla, Properties and biodegradation of thermoplastic starch obtained from grafted starches with poly(lactic acid). J. Polym. Environ. **27**, 2607-2617 (2019).
DOI: https://doi.org/10.1007/s10924-019-01540-w

[53] R. Li, Y. Wu, Z. Bai, J. Guo, X. Chen, Effect of molecular weight of polyethylene glycol on crystallization and tensile performance of polylactic acid stereocomplexes. RSC Adv. **10**, 42120-42127 (2020). DOI: https://doi.org/10.1039/d0ra08699a

[54] M. Chalid, G. Gustiraharjo, A.I. Pangesty, A. Adyandra, Y. Whulanza, S. Supriadi, Effect of PEG incorporation on physicochemical and in vitro degradation of PLLA/PDLLA blends. J. Renew. Mater. **11**, 3043-3056 (2023).
DOI: https://doi.org/10.32604/jrm.2023.026788

[55] M.S. Abdel Aziz, H.E. Salama, M.W. Sabaa, Biobased alginate/castor oil edible films for active food packaging. LWT **96**, 455-460 (2018).
DOI: https://doi.org/10.1016/j.lwt.2018.05.049

[56] C. Weerapoprasit, J. Prachayawarakorn, Properties of biodegradable thermoplastic cassava starch/sodium alginate composites prepared from injection molding. Polym. Compos. **37**, 3365-3372 (2016).
DOI: https://doi.org/10.1002/pc.23534

[57] Y. Baimark, K. Pakkethati, P. Srihanam, Properties and biodegradation of poly(lactic acid)/thermoplastic alginate biocomposites. Polymers (Basel) **17**, 1338 (2025).
DOI: https://doi.org/10.3390/polym17101338

[58] W. Thongsomboon, P. Srihanam, Y. Baimark, Preparation of flexible poly(l-lactide)-b-poly(ethylene glycol)-b-poly(l-lactide)/talcum/thermoplastic starch ternary composites. Int. J. Biol. Macromol. **230**, 123172 (2023).
DOI: https://doi.org/10.1016/j.ijbiomac.2023.123172